STANDARD ARTICLE

Journal of Veterinary Internal Medicine

Open Access

ACVIM
American College of
Veterinary Internal Medicine

Speckle tracking echocardiography in cats with preclinical hypertrophic cardiomyopathy

Ilaria Spalla [ORCID] | Adrian Boswood [ORCID] | David J. Connolly | Virginia Luis Fuentes

Clinical Science and Services, Royal Veterinary College, Hertfordshire, United Kingdom

Correspondence
Ilaria Spalla, Clinical Science and Services, Royal Veterinary College, Hawkshead Lane, North Mymms, Hatfield, Hertfordshire, AL9 7TA, United Kingdom.
Email: illispa@hotmail.com

Abstract

Background: Cats with hypertrophic cardiomyopathy (HCM) have decreased left ventricular (LV) longitudinal deformation detected by mitral annular plane systolic excursion (MAPSE) and speckle tracking echocardiography. People with preclinical HCM have decreased systolic LV longitudinal and radial strain (S) and strain rate (SR), with preserved circumferential S and SR.

Hypothesis/Objectives: Cats with preclinical HCM have decreased systolic LV deformation compared to normal cats.

Animals: Seventy-three client-owned cats with (n = 37) and without (n = 36) preclinical HCM.

Methods: Retrospective echocardiographic study. Left and right ventricular longitudinal S and SR, LV radial and circumferential S and SR were calculated by STE. Left ventricular mass was also calculated. Correlation between STE variables and LV hypertrophy was determined and receiver-operating characteristic (ROC) curves were plotted for prediction of HCM.

Results: Cats with HCM had smaller absolute longitudinal S ($-14.8 \pm 3.3\%$ vs $-19.7 \pm 2.7\%$, $P < .001$), longitudinal SR (-2.36 ± 0.62 vs -2.95 ± 0.68 second^{-1}, $P < .001$), radial S ($46.2 \pm 21.3\%$ vs $66.7 \pm 17.6\%$, $P < .001$), and radial SR (5.60 ± 2.08 vs 6.67 ± 1.8 second^{-1}, $P < .001$) compared to healthy controls. No difference was observed for circumferential S and SR. Cats with HCM had greater LV mass (13.2 ± 3.7 g vs 8.6 ± 2.7 g, $P < .001$). The ROC with the greatest area under the curve (AUC) for the identification of HCM (0.974) was plotted from a logistic regression equation combining LV mass, MAPSE at the free wall, and LV internal diameter in diastole (LVIDd).

Conclusions and clinical importance: Cats with preclinical HCM have decreased long axis and radial deformation. Decreased longitudinal deformation and decreased LVIDd are factors that would support a diagnosis of HCM.

KEYWORDS
echocardiography, feline, hypertrophic cardiomyopathy

2 | Journal of Veterinary Internal Medicine   ACVIM   SPALLA ET AL.

American College of
Veterinary Internal Medicine
Open Access

1 | INTRODUCTION

Hypertrophic cardiomyopathy (HCM) is the most common heart disease in cats, and is characterized by left ventricular (LV) hypertrophy in the absence of abnormal loading conditions.[1,2] Cats showing clinical signs have high cardiac mortality rates, but the prognosis in cats with preclinical HCM is highly variable.[3–9]

HCM is generally considered to be a disease of diastolic impairment,[10] with decreased systolic function (left ventricular fractional shortening [LVFS]) being identified as a prognostic factor in cats with HCM as a marker for late systolic impairment[8]; however, early systolic impairment occurs with reduced LV longitudinal displacement (mitral annular plane systolic excursion)[11] and longitudinal myocardial deformation (longitudinal strain) both in people and cats with HCM.[1,12–20]

Speckle tracking echocardiography (STE) allows the quantification of myocardial deformation in the longitudinal, radial, and circumferential plane and can provide information on regional and global myocardial function.[21,22] STE appears to be a sensitive technique for the early diagnosis of HCM in people, and it has been used to differentiate left ventricular hypertrophy because of HCM from athletes' heart, cardiac amyloidosis, or storage disease. STE abnormalities have been documented in people with pathogenic HCM mutations who are phenotype-negative based on conventional echocardiographic imaging.[23–28]

Reported applications for left ventricular STE in veterinary medicine have included the investigation of dilated cardiomyopathy, tachycardia-induced cardiomyopathy, degenerative mitral valve disease, and patent ductus arteriosus.[18,19,29–35] Three STE studies have reported investigations of cardiac mechanics in cats with HCM.[18,19,36] One study showed no difference in peak systolic longitudinal strain (S) and strain rate (SR) in cats with asymptomatic HCM compared to healthy controls, whereas another study showed reduced longitudinal and radial S in cats with asymptomatic HCM compared with controls. Left ventricular wall thickness was inversely correlated with longitudinal S, radial S and SR, and circumferential S and SR.[19] The most recent study investigated multilayer STE in asymptomatic cats with dynamic outflow obstruction and found lower longitudinal S and SR on all layers and an increased epicardial-to-endocardial ratio in circumferential S and SR with preserved endocardial circumferential S when compared to healthy cats.[36]

Left ventricular (LV) wall thickness is the measurement most commonly used to diagnose HCM in both people and cats; however, it is a relatively crude measure of hypertrophy and does not take into account the overall distribution. Left ventricular mass can be calculated from echocardiography and 1 study in people reported good correlation between longitudinal S and LV mass.[12,14] Left ventricular mass is not routinely obtained in cats, although 1 study reported moderate correlation between LV mass measured post-mortem (considered the gold standard) with LV mass calculated by the truncated ellipse method from 2-dimensional (2D) echocardiography in cats with HCM.[37]

Because previous STE studies in cats have enrolled relatively small, heterogeneous populations and found discordant results, we sought to investigate whether cardiac mechanics in cats with preclinical HCM were different compared to healthy control cats, and to evaluate whether the magnitude of left ventricular hypertrophy correlated with STE-derived variables. An additional aim of the study was to identify the best logistic regression model that could aid in differentiating cats with HCM from healthy controls using echocardiographic indexes other than LV wall thickness.

Our hypotheses were that longitudinal and radial S and SR would be lower in cats with HCM compared to healthy control cats, whereas circumferential S and SR would not differ. We also hypothesized that STE-derived variables would correlate with LV mass and that measurements of longitudinal deformation and LV mass would be useful in supporting a diagnosis of HCM.

2 | MATERIALS AND METHODS

The study received ethical approval from the Royal Veterinary College (SR 2018-1559). The electronic database and echocardiography records were reviewed for cats diagnosed with preclinical HCM between April 2015 and September 2017. The control group comprised mainly healthy cats undergoing cardiac assessment as part of a blood donor program or cats in which a heart murmur had been auscultated but no structural abnormalities had been identified on echocardiography.

Enrolment criteria were a complete case record (owner data, cat signalment and history, complete physical examination) and a complete echocardiographic examination. Cats were included in the preclinical HCM group if the mean left ventricular wall thickness measured at end diastole was ≥6 mm for at least 1 myocardial segment (at the interventricular septum or left ventricular free wall).[3,4,7] Cats were included in the healthy control group if no abnormalities were detected on the echocardiographic examination and no systemic illnesses that might affect hemodynamics or the cardiovascular system were observed. Additional inclusion criteria were the presence of good quality images with a minimum frame rate of 100 fps, and cine loops to allow STE evaluation from a right parasternal short axis view at the level of the papillary muscles, and a left apical 4 chamber view. Additional requirements included a symmetric, circular LV cross-section with minimal translational motion ("out-of-plane motion") for the short axis views, and long axis views excluding the LV outflow tract, optimized for LV length and endocardial borders. When available, a cine loop from the left apical view optimized for longitudinal right ventricular strain and strain rate was preferable but not necessary for inclusion in the study.

Cats were excluded if there was a history compatible with congestive heart failure; aortic thromboembolism; arrhythmias; receiving medications; diagnosis of other conditions that could affect LV wall thickness such as hyperthyroidism, systemic hypertension, acromegaly, cardiomyopathies other than HCM, congenital heart disease, or neoplastic disease. Cats were excluded for incomplete case records or an inadequate echocardiographic examination. Left atrial enlargement was not an exclusion criterion.

All echocardiographic examinations were performed using a commercial ultrasound machine with 8-12 MHz phased array ultrasound probes (Vivid E95, GE systems, Hatfield, United Kingdom).

All echocardiographic measurements represented an average of 3 measurements taken from different cardiac cine loops/still images unless stated otherwise.Mean interventricular (IVSd) and free wall (FWd) septal thickness were measured from a 2-dimensional right parasternal long axis (2D RPLax) 4-chamber view at end diastole, based on averaged thickness taken from 3 consecutive cardiac cycles. Maximal interventricular (maxIVSd) and free wall (maxFWd) thickness at end-diastole were measured as the mean value of 3 different cardiac cycles taken from the thickest segment of 3 different views: 2D RPLax 4- or 5-chambered view or a short-axis view at the papillary muscle level. End diastolic right ventricular wall thickness (RVd) was measured from the RPLax 4-chamber view at end-diastole. Left ventricular internal diameter in diastole (LVIDd) was also measured at end diastole as an average from 3 2D RPLax 4-chamber view cine loops. A leading edge to leading edge technique was used for IVSd, FWd, maxIVSd, maxFWd, RVd, and LVIDd. Left atrial size was assessed as left atrium to aorta ratio (LA/Ao), which was measured from the right parasternal short axis view at the level of the heart base optimized for the left atrium with a trailing edge to leading edge technique in the first frame after aortic valve closure.[7,10] Additionally, left atrial diameter in long axis was measured from a right parasternal 4-chamber long axis view by drawing a line parallel with the mitral annulus bisecting the left atrium in the last frame before mitral valve opening.[7] Left atrial fractional shortening (LAFS) and left ventricular fractional shortening (LVFS) were measured with a leading edge to leading edge method from M-Mode views of right parasternal short axis view at the level of the heart base and papillary muscle, respectively, as previously described.[7,38]

The area-length method from the left apical 4-chamber view was used to calculate left ventricular ejection fraction.[38,39] LV mass was calculated by the truncated ellipse method recommended in people and previously applied in cats,[37] with the apical 4-chamber view as the reference long axis view.[39]

Mitral annular plane systolic excursion at the level of the free wall (MAPSE FW) and interventricular septum (MAPSE IVS), as well as tricuspid annular plane systolic excursion (TAPSE) were measured as described.[11]

Speckle tracking postprocessing was performed off-line by 1 single, trained observer (IS). Commercial software was used for off-line analysis (Echo Pac off-line measurement software, GE systems, Hatfield, United Kingdom). The cine loop was evaluated frame by frame to select a single frame as a starting point. Generally, the software would automatically select end-systole, but the observer assessed the whole cycle before selecting the best still frame. The endocardium was tracked manually, after which a region of interest was generated by the software, and was adjusted to fit the LV wall thickness by the observer. The software automatically divided the myocardium into 6 segments and evaluated tracking quality during the cardiac cycle. The whole cine loop was further evaluated by the operator and adjusted, if needed; only 1 manual attempt to adjust endocardial points was considered acceptable. After this procedure, S and SR curves were obtained by the software. Data were then exported to an Excel data sheet and prepared for statistical analysis.

All echocardiographic values were measured 3 times on a single day by the same operator based on a single-cycle clip/image and the results shown are averaged. For advanced echocardiographic values, a global peak systolic S and SR are provided, which are the averaged value of the 6 regional segments identified by the software. Global IVS and global LVFW S and SR were also calculated as the mean value of the 3 segments belonging to the IVS or FW. Right ventricular longitudinal S and SR were calculated only at the RV free wall (3 segments) by using a LV 4 chamber template and the interventricular values were discarded. Circumferential and radial S and SR were measured from the right parasternal short axis view, whereas LV longitudinal S and SR were measured at the apical 4-chamber view, RV longitudinal S and SR, when available, from a left apical view optimized for the RV. All S and SR values were obtained from a mid-myocardium level. A within-day and between-day coefficient of variation (CV) of both global and regional strain and strain rate was assessed in 10% of the cats.

2.1 | Statistical analysis

Data were analyzed by a commercially available statistical software (IBM SPSS Statistics version 22, IBM [UK] Ltd, Portsmouth, UK) and statistical significance was set at $P < .05$. Continuous data were normally distributed according to the Shapiro-Wilk test. Data were therefore presented as mean ± SD, except for body condition score, which is an ordinal variable and was presented as median (range). In order to compare healthy control cats with affected, a t-test was used for continuous variables, a chi-squared test was performed for categorical variables, and Mann Whitney U test was applied for ordinal variables.

For the repeatability study, within-day and between-day coefficients of variation (CV) were calculated, including global and regional CV. CV was calculated as the ratio between SD and mean × 100.

Correlations between STE-derived variables and left ventricular wall thickness were tested by the Pearson's correlation coefficient. The correlation was considered perfect, strong, moderate or weak when the value of the correlation coefficient (r) was 1, 0.7-0.9, 0.4-0.6, or 0.1-0.3, respectively.[40] A receiver-operating characteristic (ROC) curve with HCM (Y/N) as the predicting factor was performed to identify the echocardiographic variables that would best classify cats with HCM by methods other than left ventricular wall thickness (gold standard). The area under the curve (AUC) was considered excellent if the AUC was between 0.90 and 1, good for 0.80-0.90, fair for 0.70-0.80 and poor for 0.60-0.70.[41] Cutoffs were also calculated and the Youden Index: ([sensitivity + specificity] − 1) was calculated to aid in the identification of the optimal cutoff.

A binary logistic regression model with the presence of HCM (Y/N) as the dependent variable was constructed. Potential explanatory variables were chosen using the values obtained from the ROC analysis of all echocardiographic variables for which there were no missing values. Variables with 95% confidence intervals for the AUC that did not include the value 0.5 were considered for entry into the model. The model was constructed in a forward stepwise manner. Variables with the highest AUC were entered into the model first and subsequent variables entered in descending order of AUC.

Improvement of the model at each step was indicated by an increase in the proportion of cases classified correctly. No more than 4 explanatory variables were entered in the model at any one time. In the final model, only variables with $P < .05$ were retained. The sensitivity of the final model to inclusion of previously excluded variables was evaluated by individually adding back all excluded variables into the final model. All variables entered into the model were checked for the risk of collinearity. No pair of independent variables had an r-value of greater than 0.8 in the correlation matrix. Goodness of fit of the model was assessed using the Hosmer and Lemeshow test.

Predicted probabilities derived from the equation generated by the final logistic regression model were used to plot an additional ROC curve.[42]

3 | RESULTS

After case selection based on the inclusion criteria (Figure 1), the final study population consisted of 73 cats: 36 healthy controls and 37 cats with preclinical HCM. Mean age was 5.1 ± 3.5 years and mean body
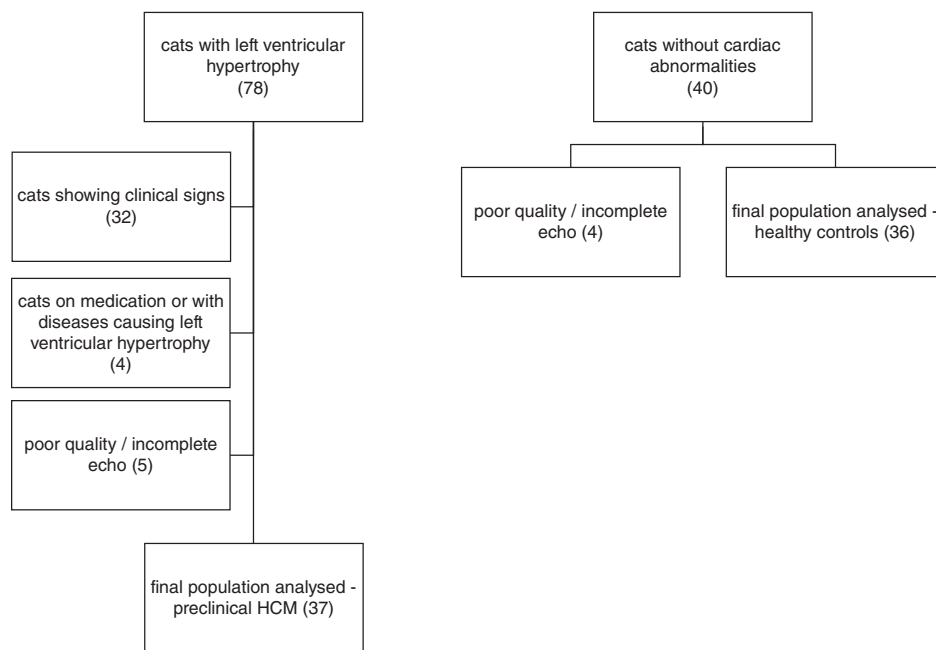

FIGURE 1 Flow diagram showing the selection process for cats with HCM and healthy controls based on the inclusion criteria. HCM, hypertrophic cardiomyopathy

TABLE 1 Baseline demographics of asymptomatic cats with HCM and healthy controls

	Healthy controls (n = 36)	HCM (n = 37)	P value
Age (years)	5 ± 3.4	5.3 ± 3.7	0.75
Sex (% male)	75% (27/36)	70% (26/11)	0.47
Breed (% non-pedigree)	69.4% (25/36)	56.7% (21/37)	0.27
Weight (kg)	4.7 ± 1.1	4.5 ± 1.1	0.48
Body condition score (1-9)	5 (3-8)	5 (2.5-7)	0.96

Data presented as mean ± SD or as a percentage (for categorical data), or median (range) for ordinal variable (body condition score). To identify any difference between groups, T-test was performed for continuous variables, chi-square for categorical variables, and Mann-Whitney-U test for ordinal variables.

TABLE 2 Coefficient of variation for global and regional speckle tracking echocardiography variables

	Circ S	Circ SR	Rad S	Rad SR	Long S	Long SR	RV Long S	RV Long SR
Global within day	4%	6%	11%	13%	4%	6%	5%	10%
Global between day	5%	8%	9%	7%	4%	6%	4%	12%
Regional within day	9%	12%	12%	11%	8%	14%	6%	15%
Regional between day	9%	13%	13%	15%	11%	16%	11%	17%

Abbreviations: Circ S, circumferential strain; Circ SR, circumferential strain rate; Long S, longitudinal strain; Long SR, longitudinal strain rate; Rad S, radial strain; Rad SR, radial strain rate; RV Long S, right ventricular longitudinal strain; RV Long SR, right ventricular longitudinal strain rate.
Coefficient of variation for advanced echocardiographic parameters.

weight was 4.6 ± 1.2 kg with no difference between groups. Most cats were male (54/73), with no difference in proportion of male cats in the 2 groups. The majority of cats were domestic shorthair (46/73),

followed by domestic longhair (6/73), Maine Coon, Sphynx and British Shorthair (5/73 each), Bengal (4/73), Devon Rex (3/73), Russian White and Ragdoll (2/73 each). No difference between the proportion of pedigree/ non-pedigree cats was found in the 2 groups (Table 1).

Within-day and between-day CV of STE-derived variables showed overall acceptable results, with greater variability on the regional S and SR compared to global S and SR (Table 2).

TABLE 3 Standard echocardiographic variables in asymptomatic cats with HCM and healthy controls

Clinical and echocardiographic parameters	Healthy controls (n = 36)	HCM (n = 37)	P value for comparison between groups
Heart Rate (bpm) n = 73	179 ± 25	179 ± 28	.99
IVSd (mm) n = 73	4.3 ± 0.4	6.8 ± 0.8	N/A
LVFWd (mm) n = 73	4.3 ± 0.5	6.3 ± 1.3	N/A
Max IVSd (mm) n = 73	4.5 ± 0.5	7.3 ± 0.8	N/A
Max LVFWd (mm) n = 73	4.3 ± 0.6	6.5 ± 1.3	N/A
LVIDd (mm) n = 73	14.9 ± 1.9	12.4 ± 1.9	<.001
RVd (mm) n = 73	2.1 ± 0.4	2.5 ± 0.4	<.001
LAD (mm) n = 73	14.1 ± 1.59	15.4 ± 2.7	.022
LA/Ao n = 73	1.23 ± 0.20	1.32 ± 0.27	.093
LAFS (%) n = 73	33.2 ± 5.6	28.8 ± 7.5	.006
LVFS (%) n = 73	48.5 ± 7.4	54.2 ± 10.1	.008
LVEF (%) n = 73	63.4 ± 8.5	65.3 ± 12.1	.45
MAPSE FW (mm) n = 73	5.5 ± 1.0	4.1 ± 0.8	<.001
MAPSE IVS (mm) n = 73	5.1 ± 0.9	4.2 ± 0.9	<.001
TAPSE (mm) n = 72	8.7 ± 1.7	7.9 ± 1.4	.028
LV mass (gr) n = 73	8.6 ± 2.7	13.2 ± 3.7	<.001

Abbreviations: IVSd, mean end-diastolic interventricular septal thickness; LA:Ao, left atrium to aorta ratio; LAD, left atrial diameter in long axis; LAFS, left atrial fractional shortening; LVEF, left ventricular ejection fraction; LVFS, left ventricular fractional shortening; LVFWd, mean end-diastolic left ventricular wall thickness; LVIDd, end diastolic left ventricular internal diameter; MAPSE FW, mitral annular plane systolic excursion measured at the free wall; MAPSE IVS, mitral annular plane systolic excursion measured at the interventricular septum; maxIVSd, maximal end-diastolic interventricular septal thickness; maxLVFWd, maximal end-diastolic left ventricular wall thickness; N/A, statistical analysis not applicable (criteria used for the classification into healthy/HCM); RVd, end diastolic right ventricular wall thickness; TAPSE, tricuspid annular plane systolic excursion; LV mass, end diastolic left ventricular mass.
Data are presented as mean ± SD. Independent t-test analysis was performed to identify difference between groups.

TABLE 4 Speckle-tracking echocardiography (STE) variables

STE	Healthy controls (n = 36 for all observations except for RV S/SR)	HCM (n = 37 for all observations except for RV S/SR)	P value for between group comparisons
Circumferential S (%)	−23.2 ± 3.9	−21.2 ± 6.2	.12
Circumferential S (%)			
IVS	−22.4 ± 5.2	−19.2 ± 6.5	
FW	−23.9 ± 4.4	−23.3 ± 7.2	
Circumferential SR (s⁻¹)	−3.84 ± 0.94	−3.73 ± 1.01	.25
Circumferential SR (s⁻¹)			
IVS	−3.75 ± 1.03	−3.58 ± 1.23	
FW	−4.01 ± 0.99	−3.9 ± 0.95	
Radial S (%)	66.7 ± 17.6	44.0 ± 21.3	<.001
Radial S (%)			
IVS	67.6 ± 18.5	44.3 ± 19.7	
FW	65.9 ± 17.5	43.7 ± 18.3	
Radial SR (s⁻¹)	6.67 ± 1.8	5.6 ± 2.08	.022
Radial SR (s⁻¹)			
IVS	6.56 ± 1.79	5.68 ± 2.45	
FW	6.80 ± 1.86	5.53 ± 1.86	
Longitudinal S (%)	−19.7 ± 2.74	−14.8 ± 3.3	<.001
Longitudinal S (%)			
IVS	−23.1 ± 3.3	−17.9 ± 3.9	
FW	−16.22 ± 3.5	−11.7 ± 4.3	
Longitudinal SR (s⁻¹)	−2.9 ± 0.68	−2.36 ± 0.62	<.001
Longitudinal SR (s⁻¹)			
IVS	−3.32 ± 0.81	−2.79 ± 0.75	
FW	−2.60 ± 0.78	−1.94 ± 0.66	
RV Longitudinal S (%) (n = 48)	−26.2 ± 5.4 (n = 24)	−26.7 ± 6.0 (n = 24)	.76
RV Longitudinal SR (s⁻¹) (n = 48)	−4.17 ± 0.88 (n = 24)	−4.66 ± 0.88 (n = 24)	.30

Abbreviations: Circumferential S, circumferential strain; Circumferential SR, circumferential strain rate; longitudinal S, left ventricular longitudinal strain; longitudinal SR, left ventricular longitudinal strain rate; Radial S, radial strain, Radial SR, radial strain rate; RV longitudinal S, right ventricular strain, RV longitudinal SR, right ventricular strain rate.
Data are presented as mean ± SD.
Independent t-test analysis was performed to identify difference between groups.

Twenty-eight cats with preclinical HCM had dynamic left ventricular outflow tract obstruction. When evaluating echocardiographic data, cats with HCM had increased left atrial diameter in long axis (LAD, $P = .002$), LVFS ($P = .008$), and LV mass ($P < .001$) compared to healthy controls. Furthermore, cats with HCM had lower LAFS ($P = .006$), MAPSE IVS ($P < .001$), MAPSE FW ($P < .001$), and TAPSE ($P = .028$) compared to healthy control cats (Table 3). When compared to normal cats, cats with HCM had lower radial S ($P < .001$) and SR ($P = .022$) and less negative longitudinal S ($P < .001$) and SR ($P < .001$) (Table 4), whereas no difference was observed for circumferential S ($P = .12$) and SR ($P = .25$) or RV longitudinal S ($P = .76$) and SR ($P = .30$).

When analyzing correlations between STE and left ventricular hypertrophy, Pearson correlation's coefficient showed moderate correlation between maximal IVS and FW thickness and the respective global IVS and FW longitudinal S ($r = 0.659$, $P < .001$ and $r = 0.524$, $P < .001$), moderate correlation between maximal IVS and FW and the respective global IVS and FW radial strain ($r = -0.494$, $P < .001$ and $r = -0.413$, $P < .001$). Weak correlation was observed for maximal IVS and FW thickness and the respective global IVS and FW longitudinal

SR ($r = 0.327$, $P = .005$ and $r = 0.371$, $P = .001$) as well as maximal IVS and global IVS circumferential S ($r = 0.307$, $P = .008$).

Left ventricular mass was strongly correlated with IVSd and LVFWd ($r = 0.701$, $P < .001$ and $r = 0.715$, $P < .001$ respectively). Additionally, LV mass moderately correlated with longitudinal S and SR ($r = 0.511$, $P < .001$ and $r = 0.311$, $P = .007$, respectively), but not with other STE-derived variables. No significant correlation was found between body weight and LV mass or longitudinal S or SR. No significant correlation was found between heart rate and STE-derived variables.

When assessing the predictive ability of STE-derived variables, LV mass and standard echocardiographic variables, the ROC curves showed that LV mass, and longitudinal S had some of the highest AUCs of 0.867 (CI: 0.783-0.951) and 0.862, respectively (CI:0.781-0.943) (Figure 2, Table 5). Based on the Youden Index, the best cutoff for LV mass was 10 g (Youden Index 0.62) and −15.9% for Long S (Youden index 0.56).

The final logistic regression model showed that LV mass, MAPSE FW, and LVIDd in combination best predicted the presence of HCM (Table 6).

The combination of these tests increased the probability of a cat with HCM to be correctly classified as affected (predicted ROC curve, AUC 0.974, CI 0.945-1.000) (Figure 2).
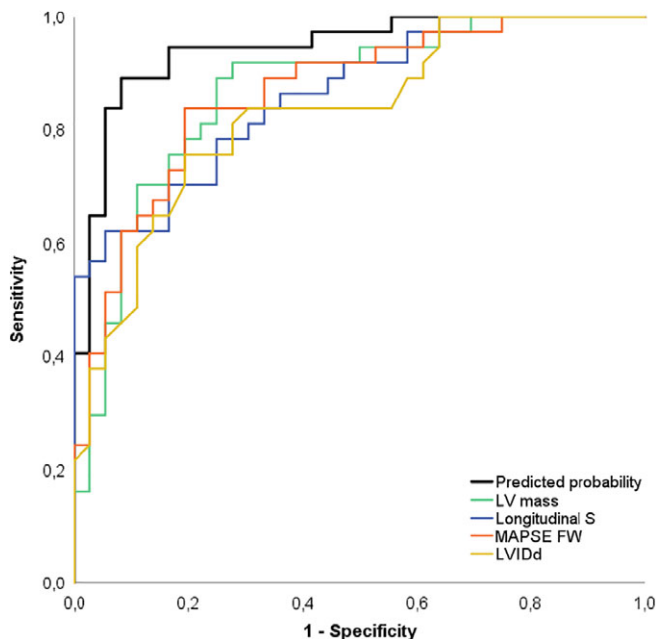

FIGURE 2 ROC curve constructed using probabilities derived from the binary logistic regression and selected echocardiographic variables to differentiate asymptomatic cats from those with HCM. The 4 individual echocardiographic variables with the greatest areas under the curve are plotted in addition to the predicted probabilities from the regression equation. The gold standard was 2-dimensional left ventricular wall thickness. The area under the curve with 95% confidence interval values is displayed in Table 5. Predicted probability, derived from binary logistic regression model; LV mass truncated ellipsoid, end-diastolic left ventricular mass measured by the truncated ellipse method; longitudinal S, left ventricular longitudinal strain; MAPSE FW, mitral annular plane systolic excursion measured at the free wall; LVIDd, end diastolic left ventricular internal diameter

TABLE 5 Output from ROC curves

Variable	Area under the curve (AUC)	95% CI
Predicted model	0.974	0.945-1.000
LV mass	0.867	0.783-0.951
MAPSE FW	0.864	0.781-0.947
Longitudinal S	0.862	0.781-0.943
LVIDd	0.827	0.734-0.921
RVd	0.803	0.699-0.907
Radial S	0.788	0.682-0.895
MAPSE IVS	0.784	0.638-0.858
Longitudinal SR	0.751	0.639-0.862
LAFS	0.681	0.556-0.805
LVFS	0.673	0.548-0.798
Radial SR	0.655	0.528-0.782
LAD	0.651	0.523-0.779
TAPSE	0.627	0.495-0.758
LA/Ao	0.610	0.480-0.741
EF	0.584	0.450-0.718
Circumferential S	0.577	0.444-0.710
Circumferential SR	0.521	0.387-0.655
RV Longitudinal S	0.483	0.319-0.648
RV Longitudinal SR	0.446	0.282-0.611

Output from ROC curves for echocardiographic variables and predicted probabilities obtained from multivariable logistic regression analysis. Area under the curve (AUC) and 95% confident interval (CI) are provided.

TABLE 6 Binary logistic regression analysis results

Parameter	B value	OR	CI	Wald	P value
LV mass	0.792	2.207	1.435-3.395	12.99	<.001
LVIDd	−0.681	0.506	0.287-0.891	5.569	=.018
MAPSE FW	−1.524	0.218	0.060-0.792	5.352	=.021
Constant	8.385	4381.982		5.057	=.025

Abbreviations: B value, beta value coefficient; CI, confident interval; LV mass, end diastolic left ventricular mass; LVIDd, end diastolic left ventricular internal diameter; OR, odds ratio; MAPSE FW, mitral annular plane systolic excursion measured at the free wall, which were all statistically significant in the model; Wald, wald test result.

4 | DISCUSSION

The results of the present study showed that in 2 groups of cats of similar age, sex, weight, body condition score, and heart rate, cats with preclinical HCM had lower absolute values of both longitudinal and radial S and SR, and greater LV mass. Furthermore, a correlation was found between regional IVS or FW longitudinal S and regional LV wall thickness, as well as between longitudinal S or SR and LV mass. In the study population, these variables performed well individually at differentiating cats with preclinical HCM from controls when compared to standard echocardiographic variables. The logistic regression model that best predicted the presence of HCM included a combination of LV mass, MAPSE FW, and LVIDd. Within-day and between-day CV was acceptable and similar to previous studies,[34,35,43] with global S and SR values achieving better reproducibility than regional measurements, as identified in a previous study on S/SR.[43]

Studies on myocardial fiber distribution showed that the myocardium has longitudinally and circumferentially oriented fibers, which support cardiac contraction in different deformation planes.[44] Short axis, long axis, and twist represent deformation planes that contribute to cardiac ejection.[22] LVFS can be considered a surrogate of short axis deformation, as well as circumferential and radial S and SR. Long axis function can be identified by atrioventricular systolic plane excursion (MAPSE), as during contraction the cardiac base descends toward the cardiac apex[45]; longitudinal S and SR are also additional long axis deformation variables. The right ventricle has mainly longitudinally oriented fibers, with minimal short axis deformation, therefore TAPSE and longitudinal S and SR are the deformation variables that can be used to assess right ventricular deformation. Torsion and twist are an additional feature of the contracting heart, as the heart base and apex counter-rotate to allow twisting of the left ventricle to aid ejection.

STE allows the evaluation of myocardial deformation in different planes and is an echocardiography-based technique.[21,22] As with every technique, there are limitations, which for STE are mainly related to image quality, out of plane motion, and load dependency.[21] Additional limitations include a steep learning curve, inter-vendor software analysis variation and an overall acceptable CV, mainly with global results, yet regional segment analysis can have greater variation (up to 16% of variation).[43] The present study included cases seen at the authors' outpatient clinic, and the required cine loops were not different from the standard views required for a standard echocardiogram. It is important to take particular care with image quality, symmetry and in limiting out-of-plane motion to allow STE analysis and this technique might therefore be difficult in uncooperative or critically ill cats.

The results of our study showed that longitudinal deformation is impaired early in the disease, similar to previous reports in people with preclinical HCM[13–17] where early impairment in longitudinal and radial S and SR has been observed, whereas circumferential S and SR tend to be preserved or increased, with some studies reporting deterioration of the circumferential deformation as a possible explanation for the development of clinical signs.[12,14,16]

Previous studies assessing STE in cats with HCM showed discordant results. One study did not identify any change in longitudinal systolic S or SR, with the only abnormality detected being a diastolic change in longitudinal E and A SR, but not its ratio.[18] The cat population was relatively homogeneous and no cat received treatment. However, sample size was smaller than our study, and the degree of hypertrophy was mild, which might account for the differences in the results. Also, no segmental S or SR data were shown, and only global values were presented. In the present study, diastolic SR analysis was not performed so it is not possible to fully compare our study to those previously published. Another study reported decreased radial and longitudinal systolic S and SR in cats with HCM not showing clinical signs and with congestive heart failure, but not in those showing clinical signs other than CHF (exercise intolerance, dyspnea or tachypnea).[19] The multiple subgroups with low number of cats in each group could have limited statistical power. No characterization on hypertrophy distribution and regional mechanics was mentioned in that study,[19] and cardiac therapy was allowed. Our results confirm the previous observation that cats with asymptomatic HCM have lower absolute values of longitudinal and radial deformation compared to healthy cats. A more recent study identified preserved endocardial circumferential strain but lower epicardial values resulting in greater epicardial to endocardial ratio in cats with dynamic outflow tract obstruction and HCM,[36] so it could be that more detailed analysis of circumferential deformation would be required in the assessment of cats with HCM. Compared with healthy control cats, the cats with preclinical HCM in our study had decreased longitudinal and radial deformation with similar circumferential S and SR, that was assessed at the mid-myocardium level, in contrast to the previously cited study,[36] where the whole layer circumferential results were lower in asymptomatic cats with HCM, but were not statistically different on a previous study from the same group.[19] There are similar discrepancies

in circumferential S and SR in humans[12,14,16] and there is currently interest in the assessment of a transmural strain difference both on MRI and echocardiography[46,47] in human cardiology.

The best correlation with regional hypertrophy and left ventricular mass was observed with longitudinal S and SR. No weight-dependence was identified in the present study in STE-derived values, although the weight range in our group of cats was relatively narrow, with few cats weighing more than 5 kg or less than 3 kg. A similar lack of correlation between LV mass and bodyweight was also observed. The present findings suggest that in this population of cats, STE and LV mass can provide a weightless index to aid in the characterization of HCM; however, further studies are required to elucidate if a wider body weight range would impact LV mass and STE variables based on the findings of increasing LV wall thickness with increasing body weight.[48]

LV mass has been quantified by MRI, echocardiography and post-mortem in cats[37]; however, no extensive use of this technique has been applied in veterinary medicine. To the author's knowledge, no repeatability studies in the veterinary literature are available. Different LV mass calculations in people are available, including M-mode and 2D based calculations. The truncated ellipse method is the 2-dimensional method recommended in human guidelines[39] and previously applied in cats.[37] It requires both short- and long-axis views, but an overall acceptable correlation was found compared to post-mortem LV mass assessment in cats, although MRI-based mass calculation correlated better to actual LV mass.[37] Healthy control cats in our study had similar values to the ones reported previously.[37] Longitudinal S and SR seemed to correlate well with LV mass, with less negative longitudinal S values associated with increasing LV mass. There is similar correlation in people with HCM.[12,14]

Early diagnosis and risk stratification are important targets in human medicine in order to deliver the best treatment options. A decrease in longitudinal S has been associated with a poorer prognosis in people, with the highest incidence of adverse events (including congestive heart failure, ventricular tachycardia, sudden cardiac death or the implantation of a cardiodefibrillator device) with lower absolute values (ie, less negative results).[49] A longitudinal S greater than −16% (ie, less negative) was an independent predictor of adverse effects in people.[50] Longitudinal S could be of help in classifying equivocal or challenging cases or allow a closer monitoring over time; however, longitudinal studies are required to investigate this aspect. Because of the previously reported limitations in the technique and the results of our regression analysis, MAPSE seems to be a more widely applicable alternative in the assessment of longitudinal deformation, with the main limitation of this technique associated with the specific regional sampling required (atrioventricular annulus and not a global index of longitudinal deformation).

The logistic regression model that showed the best association with a diagnosis of HCM in our population combined LV mass, MAPSE FW, and LVIDd. When left ventricular hypertrophy is manifest, left ventricular wall thickness is likely sufficient to discriminate between affected and non-affected. However, combining different variables could help in settings where the hypertrophy is not as obvious, such as in equivocal cases or in cats with a family history of HCM. Interestingly, the 3 variables that were shown to increase the probability of a cat to have HCM include a marker of global wall thickness (LV mass), LV chamber size, and longitudinal deformation. This might indicate that alongside wall thickness, LV geometry and function are additional tools that could aid identifying HCM or improve monitoring. This potential application requires further investigation. Longitudinal observational studies in cats with preclinical HCM and with equivocal HCM might provide insight into the applicability of longitudinal S or MAPSE and LV mass as an aid in risk stratification for HCM development or progression. Genotype-positive and phenotype-negative people represent a challenge in human cardiology, and few studies have investigated abnormalities using advanced echocardiographic techniques.[27,28] Maine Coon cats heterozygous for the mutation A31P do not always show LV hypertrophy[51-55] but the prevalence of hypertrophy increases with age[53,55] so use of a combined predictive model would be worth evaluating in this context.

As expected, cats with HCM had thicker end-diastolic RV wall thicknesses values as previously identfied.[56,57] Interestingly, in the asymptomatic phase, no difference in RV Long S and SR was observed. TAPSE values are lower in cats with CHF, so it could be possible that RV global long axis deformation is impaired later on, when clinical signs develop or when there is an increase in pulmonary arterial pressure or pulmonary hypertension.[58]

Limitations of the present study include its retrospective nature; however, a standardized protocol for clinical cats and healthy controls was applied. It was not possible to blind the operator to the presence of LV hypertrophy when making echocardiographic measurements, and our study did not address diastolic function deformation via standard echocardiography or STE, or torsion or twist. Variability of right ventricular shape makes RV imaging more challenging; where available, the authors used RV focused views; otherwise, RV S and SR were not assessed. Our study was not designed to assess genotype. The classification and ROC curve output was based on a 2D end-diastolic LV wall thickness cutoff of 6 mm, which is considered a conservative cutoff for the diagnosis of HCM in cats, it is possible that other cutoffs could be better at classifying HCM in cats. Furthermore, the authors cannot exclude that the healthy cats group might have included cats with preclinical HCM not meeting the current criteria for HCM. Additionally, the regression model was performed in a dichotomous population of cats, where LV hypertrophy was manifest or absent based on the selected cutoff, so the results of this model might not be readily applied in a population of cats with equivocal/genotype positive-phenotype negative cats, for which a longitudinal study would be required.

In conclusion, cats with HCM had decreased systolic long axis deformation and radial deformation, but overall preserved circumferential deformation. Left ventricular mass was increased in cats with HCM. LV mass and longitudinal S correlated with the degree of left ventricular hypertrophy and performed best when compared to standard echocardiographic variables. STE CV was acceptable, with the lowest CV with global S and SR. Longitudinal S and LV mass might be useful additional variables in the evaluation of cats with HCM.

CONFLICT OF INTEREST DECLARATION

Authors declare that they have no conflict of interest with the contents of this article.

OFF-LABEL ANTIMICROBIAL DECLARATION

Authors declare no off-label use of antimicrobials.

INSTITUTIONAL ANIMAL CARE AND USE COMMITTEE (IACUC) OR OTHER APPROVAL DECLARATION

Royal Veterinary College IACUC approval, SR 2018-1559.

HUMAN ETHICS APPROVAL DECLARATION

Authors declare that human ethics approval was not needed for this study.

ORCID

Ilaria Spalla https://orcid.org/0000-0003-0039-1438
Adrian Boswood https://orcid.org/0000-0003-1795-4364

REFERENCES

1. Elliot P, Andersson B, Arbustini E, et al. Classification of the cardiomyopathies: a position statement from the European society of cardiology working group on myocardial and pericardial diseases. *Eur Heart J*. 2006;29:270-276.
2. Payne JR, Brodbelt DC, Luis Fuentes V. Cardiomyopathy prevalence in 780 apparently healthy cats in rehoming centres (the CatScan study). *J Vet Cardiol*. 2015;17(S1):S244-S257.
3. Payne JR, Luis Fuentes V, Boswood A, Brodbelt D. Population characteristic and survival in 127 referred cats with hypertrophic cardiomyopathy (1997 to 2005). *J Small Anim Pract*. 2010;51:540-547.
4. Trehiou-Sechi E, Tissier R, Gouni R, et al. Comparative echocardiographic and clinical features of hypertrophic cardiomyopathy in 5 breeds of cats: a retrospective analysis of 344 cases (2001-2011). *J. Vet. Int. Med*. 2012;26:532–541.
5. Lefbom BK, Rosenthal SL, Tyrrell WDJ, et al. Severe hypertrophic cardiomyopathy in 10 young Ragdoll cats. *J Vet Intern Med*. 2001; 15:308.
6. Rush JE, Freeman LM, Fenollosa LK, et al. Population and survival characteristics of cats with hypertrophic cardiomyopathy: 260 cases (1990-1999). *J Am Vet Med Assoc*. 2002;220:202-207.
7. Payne JR, Borgeat K, Connolly DJ, et al. Prognostic indicators in cats with hypertrophic cardiomyopathy. *J Vet Intern Med*. 2013;27:1427-1436.
8. Payne JR, Borgeat K, Brodbelt DC, et al. Risk factors associated with sudden death vs. congestive heart failure or arterial thromboembolism in cats with hypertrophic cardiomyopathy. *J Vet Cardiol*. 2015;S1: S318-S328.
9. Fox PR, Keene BW, Lamb K, et al. International collaborative study to assess cardiovascular risk and evaluate long-term health in cats with preclinical hypertrophic cardiomyopathy and apparently healthy cats: the REVEAL Study. *J Vet Intern Med*. 2018;32(3):930-943.
10. Schober KE, Chetboul V. Echocardiographic evaluation of left ventricular diastolic function in cats: hemodynamic determinants and pattern recognition. *J Vet Cardiol*. 2015;17(Suppl 1):S102-S133.
11. Spalla I, Payne JR, Pope A, et al. Mitral annular plane systolic excursion and tricuspid annular plane systolic excursion in cats with hypertrophic cardiomyopathy. *J Vet Intern Med*. 2017;31:691-699.
12. Urbano-Moral JA, Rowin EJ, Maron MS, Crean A, Pandian NG. Investigation of global and regional myocardial mechanics with 3-dimensional speckle tracking echocardiography and relations to hypertrophy and fibrosis in hypertrophic cardiomyopathy. *Circ Cardiovasc Imaging*. 2014; 7:11-19.
13. Serri K, Reant P, Lafitte M, et al. Global and regional myocardial function quantification by two-dimensional strain: application in hypertrophic cardiomyopathy. *J Am Coll Cardiol*. 2006;47:1175-1181.
14. Inciardi R, Galderisi M, Nistri S, et al. Echocardiographic advances in hypertrophic cardiomyopathy: three dimensional and strain imaging echocardiography. *Echocardiography*. 2018;35:716-726. Epub ahead of print.
15. Carasso S, Yang H, Woo A, et al. Systolic myocardial mechanics in hypertrophic cardiomyopathy: novel concepts and implications for clinical status. *J Am Soc Echocardiogr*. 2008;21:675-683.
16. Huang J, Yan ZN, Rui YF, Fan L, Liu C, Li J. Left ventricular short axis systolic function changes in patients with hypertrophic cardiomyopathy detected by two- dimensional speckle tracking imaging. *BMC Cardiovasc Disord*. 2018;18:13.
17. Voilliot D, Huttin O, Hammache N, et al. Impact of global and segmental hypertrophy on two/dimensional strain derived from three dimensional echocardiography in hypertrophic cardiomyopathy: comparison with healthy subjects. *J Am Soc Echocardiogr*. 2015;28: 1093-1102.
18. Sugimoto K, Fuji Y, Sunahara H, et al. Assessment of left ventricular longitudinal function in cats with subclinical hypertrophic cardiomyopathy using tissue Doppler imaging and speckle tracking echocardiography. *J Vet Med Sci*. 2015;77:1101-1108.
19. Suzuki R, Mochizuki Y, Yoshimatsu H. Determination of multidirectional myocardial deformations in cats with hypertrophic cardiomyopathy by using two dimensional speckle tracking echocardiography. *J Fel Med Surg*. 2017;19:1283-1289.
20. Wess G, Sarkar R, Hartmann K. Assessment of left ventricular systolic function by strain imaging echocardiography in various stages of feline hypertrophic cardiomyopathy. *J Vet Intern Med*. 2010;24: 1375-1382.
21. Mor-Avi V, Lang RM, Badano LP, et al. Current and evolving echocardiographic techniques for the quantitative evaluation of cardiac mechanics: ASE/EAE consensus statement on methodology and indications endorsed by the Japanese Society of Echocardiography. *Eur J Echocardiogr*. 2011;12:167-205.
22. Blessberger H, Binder T. Two-dimensional speckle tracking echocardiography: basic principles. *Heart*. 2010;96:716-722.
23. Collier P, Phelan D, Klein A. A test in context: myocardial strain measured by speckle-tracking echocardiography. *J Am Coll Cardiol*. 2017; 69:1043-1056.
24. Ternacle J, Bremont C, d'Humieres T, et al. Left ventricular dyssynchrony and 2D and 3D global longitudinal strain for differentiating physiological and pathological left ventricular hypertrophy. *Arch Cardiovasc Dis*. 2017;110:403-412.
25. Richand V, Lafitte S, Reant P, et al. An ultrasound speckle tracking (two-dimensional strain) analysis of myocardial deformation in professional soccer players compared with healthy subjects and hypertrophic cardiomyopathy. *Am J Cardiol*. 2007;100:128-132.
26. D'Andrea A, Radmilovic J, Ballo P, et al. Left ventricular hypertrophy or storage disease? The incremental value of speckle tracking strain bull's-eye. *Echocardiography*. 2017;34:746-759.
27. Forsey J, Benson L, Rozenblyum E, Friedberg MK, Mertens L. Early changes in apical rotation in genotype positive children with

hypertrophic cardiomyopathy mutations without hypertrophic changes on two-dimensional imaging. *J Am Soc Echocardiogr*. 2014;27:215-221.

28. Cardim N, Galderisi M, Edvardsen T. Role of multimodality cardiac imaging in the management of patients with hypertrophic cardiomyopathy: an expert consensus of the European Association of Cardiovascular Imaging Endorsed by the Saudi Heart Association. *Eur Heart J Cardiovasc Imaging*. 2015;16:280-235.

29. Pedro B, Stephenson H, Linney C, Cripps P, Dukes-McEwan J. Assessment of left ventricular function in healthy Great Danes and in Great Danes with dilated cardiomyopathy using speckle tracking echocardiography. *J Vet Cardiol*. 2017;19:363-375.

30. Kusunose K, Zhang Y, Mazgalev TN. Left ventricular strain distribution in healthy dogs and in dogs with tachycardia-induced dilated cardiomyopathy. *Cardiovasc Ultrasound*. 2013;11:43-52.

31. Zois NE, Olsen NT, Moesgaard SG, et al. Left ventricular twist and circumferential strain in dogs with myxomatous mitral valve disease. *J Vet Intern Med*. 2013;27:875-883.

32. Zois NE, Tidholm A, Nägga KM, et al. Radial and longitudinal strain and strain rate assessed by speckle-tracking echocardiography in dogs with myxomatous mitral valve disease. *J Vet Intern Med*. 2012;26:1309-1319.

33. Suzuki R, Matsumoto H, Teshima T, Koyama H. Clinical assessment of systolic myocardial deformations in dogs with chronic mitral valve insufficiency using two-dimensional speckle-tracking echocardiography. *J Vet Cardiol*. 2013;15:41-49.

34. Spalla I, Locatelli C, Zanaboni AM, Brambilla P, Bussadori C. Speckle-tracking echocardiography in dogs with patent ductus arteriosus: effect of percutaneous closure on cardiac mechanics. *J Vet Intern Med*. 2016;30:714-721.

35. Spalla I, Locatelli C, Zanaboni AM, Brambilla P, Bussadori C. Echocardiographic assessment of cardiac function by conventional and speckle-tracking echocardiography in dogs with patent Ductus Arteriosus. *J Vet Intern Med*. 2016;30:706-713.

36. Suzuki R, Mochizuki Y, Yoshimatsu H. Layer-specific myocardial function in asymptomatic cats with obstructive hypertrophic cardiomyopathy assessed using 2-dimensional speckle-tracking echocardiography. *J Vet Intern Med*. 2019;33(1):37-45.

37. MacDonald KA, Kittleson MK, Reed T, et al. Quantification of left ventricular mass using cardiac magnetic resonance imaging compared with echocardiography in domestic cats. *Vet Radiol and US*. 2005;46:192-199.

38. Boon J. Evaluation of size, function and hemodynamics. In: Boon J, ed. *Veterinary Echocardiography*. 2nd ed. Chichester, UK: Wiley Blackwell; 2011:153-266.

39. Lang RM, Badano LP, Mor-Avi V, et al. Recommendations for cardiac chamber quantification by echocardiography in adults: an update from the American Society of Echocardiography and the European Association of Cardiovascular Imaging. *Eur Heart J Cardiovasc Imaging*. 2015;16:233-270.

40. Evans JD. *Straightforward Statistics for the Behavioral Sciences*. Pacific Grove, CA: Brooks/Cole Publishing; 1996, 1996.

41. Fischer JE, Bachman LM, Jaeschke R. A readers' guide to the interpretation of diagnostic test properties: clinical example of sepsis. *Intensive Care Med*. 2003;29:1043-1051.

42. Buntix F, Aertgeets B, Aerts M, et al. Multivariable analysis in diagnostic accuracy studies: what are the possibilities? In: Knottenerus JA, Buntinx F, eds. *The Evidence Base of Clinical Diagnosis: Theory and Methods of Diagnostic Research*. 2nd ed. Chichester, UK: Wiley Blackwell; 2009:146-166.

43. Santarelli G, Talavera López J, Fernández Del Palacio J. Evaluation of the right parasternal four-chamber view for the assessment of left ventricular longitudinal strain and strain rate by two-dimensional speckle tracking echocardiography in dogs. *Res Vet Sci*. 2018 Oct;120:78-85.

44. Sosnik DE, Wang R, Dai G, et al. Diffusion MRI tractorgraphy of the heart. *J Cardiovasc Magn Reson*. 2009;11:47-62.

45. Carlsson M, Ugander M, Mosén H, Buhre T, Arheden H. Atrioventricular plane displacement is the major contributor to left ventricular pumping in healthy adults, athletes, and patients with dilated cardiomyopathy. *Am J Physiol Heart Circ Physiol*. 2007;292:H1452-H1459.

46. Sun JP, Xu TY, Ni XD, et al. Echocardiographic strain in hypertrophic cardiomyopathy and hypertensive left ventricular hypertrophy. *Echocardiography*. 2019;36:257-265.

47. Vigneault DM, Yang E, Jensen PJ, et al. Left ventricular strain is abnormal in preclinical and overt hypertrophic cardiomyopathy: cardiac MR feature tracking. *Radiology*. 2019;290:640-648.

48. Häggström J, Andersson ÅO, Falk T, et al. Effect of body weight on echocardiographic measurements in 19'866 pure-bred cats with or without heart disease. *J Vet Intern Med*. 2016;30:4601-1611.

49. Reant P, Mirabel M, Lloyd G. Global longitudinal strain is associated with heart failure outcomes in hypertrophic cardiomyopathy. *Heart*. 2016;102:741-747.

50. Hartlage GR, Kim JH, Strickland PT, et al. The prognostic value of standardized reference values for speckle-tracking global longitudinal strain in hypertrophic cardiomyopathy. *Int J Cardiovasc Imaging*. 2015;31:557-565.

51. Carlos Sampedrano C, Chetboul V, Mary J. Prospective echocardiographic and tissue Doppler imaging screening of a population of Maine Coon cats tested for the A31P mutation in the myosin-binding protein C gene: a specific analysis of the heterozygous status. *J Vet Intern Med*. 2009;23:91-99.

52. Longeri M, Ferrari P, Knafelz P. Myosin-binding protein C DNA variants in domestic cats (A31P, A74T, R820W) and their association with hypertrophic cardiomyopathy. *J Vet Intern Med*. 2013;27:275-285.

53. Godiksen M, Granstrøm S, Koch J. Hypertrophic cardiomyopathy in young Maine Coon cats caused by the p.A31P cMyBP-C mutation - the clinical significance of having the mutation. *Acta Vet Scand*. 2011;53:7.

54. Granström S, Godiksen MT, Christiansen M. Genotype-phenotype correlation between the cardiac myosin binding protein C mutation A31P and hypertrophic cardiomyopathy in a cohort of Maine Coon cats: a longitudinal study. *J Vet Cardiol*. 2015;17:S268-S281.

55. Wess G, Schinner C, Weber K. Association of A31P and A74T polymorphisms in the myosin binding protein C3 gene and hypertrophic cardiomyopathy in Maine coon and other breed cats. *J Vet Intern Med*. 2010;24:527-532.

56. Schober KE, Savino SI, Yildiz V. Right ventricular involvement in feline hypertrophic cardiomyopathy. *J Vet Cardiol*. 2016;18:297-309.

57. Visser LC, Sloan CQ, Stern JA. Echocardiographic assessment of right ventricular size and function in cats with hypertrophic cardiomyopathy. *J Vet Intern Med*. 2017;31:668-677.

58. Vezzosi T, Schober KE. Doppler-derived echocardiographic evidence of pulmonary hypertension in cats with left-sided congestive heart failure. *J Vet Cardiol*. 2019;23:58-68.